ORIGINAL PAPER

Modelling and analysis of polarization noise in vertical cavity surface emitting LASERs

Abhilash Singh[1] · Mohit Sharma[2] · Rahul Kumar[2] · Somendra Prakash Singh[2] · Jyoti Raj Madhesiya[2]

Abstract

Previous researches have provided mathematical models of vertical cavity surface emitting LASER's (VCSEL's) that evaluated the effect of spontaneous noise on the Laser's performance but completely neglected the effect of polarization noise. Also the results presented were in terms of RIN variation with respect to frequency. In this paper, a model is proposed to analyse the effect of spontaneous and polarization noise on VCSEL's output power. Spontaneous noise is included by augmenting feedback in photon rate equations. Polarization noise is incorporated in the dynamics with the help of self-stabilizing and gain recovering coefficients. Characteristics of VCSEL's output power are studied under continuous wave (CW) and sinusoidal modulation. VCSEL dynamics are simulated for both the cases with and without noise, firstly without noise and then with the effect of noise. The output light's power curves depict the effect of spontaneous and polarization noise in VCSEL. For high frequency modulation, the outputs have fluctuations throughout the simulation time but noise amplifies these fluctuations, affecting the performance of LASER. For CW modulation, the output light shows exponential behaviour with respect to bias.

Keywords VCSEL · CW modulation · Two-tone modulation · Spontaneous noise · Polarization noise

1 Introduction

In today's world all the communication network's backbone is based on fiber optic links. An optical network is comprised of three major components: optical sources, waveguides and receivers. To ensure good signal quality all these components must operate perfectly and to operate at highest efficiency all the components must be free from noise. Although every component has its own set of noise that degrades its per-formance. But in a system some noises are introduced into them through other components. In this paper, the area of interest is the noise generated by most efficient and widely used optical sources. Most efficient light source used nowa-days is VCSEL. It has some inherent qualities that promotes its usage as a light source in optical communication such as comparatively low cost, large bandwidth and high den-sity. For any system, the ability to handle noise, internal or external is of utmost importance.

Radiation of light in VCSEL is based on two principles: spontaneous emission and stimulated emission. Stimulated emission does not generate any noise of its own it just mul-tiplies the noise generated because of spontaneous emission. Hence it can be concluded that on the basis of emission principle, spontaneous emission is the only source of noise in VCSEL (Ahmed et al. 2014). Apart from spontaneous noise, VCSEL's performance is also affected due to the phenomenon of polarization. Most papers study the effect of spontaneous noise on VCSEL characteristics neglecting polarization noise. In this paper, the model incorporates both spontaneous and polarization noise in previously proposed VCSEL photon and carrier rate equations of VCSEL with the novelty of explaining the effect of polarization noise in VCSEL.

✉ Abhilash Singh
 sabhilash@iiserb.ac.in

 Mohit Sharma
 mohitsharma5722@gmail.com

 Rahul Kumar
 rahulupadhyay2k16@gmail.com

 Somendra Prakash Singh
 30singhsp@gmail.com

 Jyoti Raj Madhesiya
 raj95jyoti@gmail.com

[1] Indian Institute of Science Education and Research, Bhopal, India

[2] School of ICT, Gautam Buddha University, Greater Noida, India

For supporting multiple modes, VCSEL's cavity length is increased and it is comparatively larger as compared to edge emitting LASERs (Ahmed et al. 2014). With increase in cavity size, the spatial distribution of carriers comes into play and it affects the output light at different modes. This phenomenon of spatial heterogeneity is known as spatial hole burning. For increasing the transmission of light at a particular wavelength, absorption of photons at that wavelength is reduced to increase the transmission of photons particularly at that wavelength. This phenomenon is known as spectral hole burning. With increase in the number of simultaneous modes, the signal from adjacent modes acts as a noise to other nodes. Hence, operating frequencies of adjacent modes need to be separated by a guard band to ensure that the signals don't interfere with one another. In a LASER, the most prominent characteristic of output light is its coherence, the photons in the output of a LASER are similar in amplitude and phase. The phenomenon explained in this paragraph alter these characteristics of VCSEL. Hence keeping an eye on their effect on VCSEL would provide us a better understanding of the functioning of VCSEL and the noise present in it. With the help of this study, LASER based system designers would be able to choose appropriate modulation conditions giving best performance.

In 1985, Chen et al. studied the polarization bistablity switching mechanisms in VCSELs for two mode VCSEL (Chen and Liu 1987). In 1994, Choquette et al. shows that the polarization characteristics of VCSEL are related to optical resonance of temperature dependent cavity and spectral alignment of LASER gain (Choquette et al. 1994). In 1995, Mukaihara et al. investigates the additional noise characterized due to polarization fluctuations in InGaAs-GaAs VCSEL. Intensity noise gets increased due to polarization distortions, even in the case of single transverse mode. The operating temperature and injection current make the polarization states unstable (Mukaihara et al. 1995). In 1997, Law et al. presented a numerical study to understand effect of spatial hole burning and diffusion of carriers on the noise characteristics of VCSEL operating in single mode and multimode (Lee and Ram 2001). In 2005, Gatare et al. experimentally and theoretically studied the polarization dynamics of VCSEL when subjected to optical injection (Gatare et al. 2005). In 2011, Quirce et al. experimentally investigated the noise characteristics of multimode VCSEL emitting at around 1560nm wavelength. This paper shows that the noise characteristics change when polarization instabilities are considered (Quirce et al. 2011). In 2012 Ahmed et al. investigated the characteristics of VCSEL when subjected to sinusoidal modulation. This paper studies the half and higher harmonic distortions in the LASER (Ahmed and Yamada 2012). In 2013 Mahmoud et al. showed extensive numerical simulations for modulation characteristics of VCSEL subjected to analog modulation over modula-

tion index and modulation frequency. It studies nonlinear characteristics of VCSEL by evaluating harmonic response and harmonic distortion under CW modulation, single-tone modulation and two tone modulation. It says that distortions are present due to modulation and relaxation frequencies (Mahmoud et al. 2013). In 2014, Ahmed et al. presents the numerical simulations of the dynamics and noise of directly modulated VCSEL as primary light sources in RF links. RF link's Noise Figure is evaluated to determine the effect of noise generated by VCSEL on the noise performance of the RF link (Ahmed et al. 2014). In 2016, Priyanka et al. presents the simulation results and DC characteristic analysis of GaAs/InGaAs VCSEL for the third transparent window wavelengths. The active region used in the simulated LASER is InGaAsP (Priyanka et al. 2016).

In this paper, the dynamics of VCSEL is augmented with the different types of noises. The results are obtained in terms of output power and time. The output power is calculated for different modes inside a VCSEL with and without noise. The VCSEL dynamics are simulated under CW operation and two-tone modulation. This research would then offer assistance laser-based framework designers to pick the modulation conditions giving best noise performance.

The paper is organized as follows. In Sect. 2, the photon and carrier rate equations of VCSEL oscillating in two modes with augmented Langevin noise sources and polarization parameters are presented with details about the modulation of input bias and also elaborates the evaluation procedures of the rate equations. Section 3 present the results and their analysis. Section 4 presents the conclusions derived from the paper.

2 Theoretical model

In this section, the dynamics of VCSEL is described to study and analyze VCSEL characteristics. Written below are the rate equations used to determine the fluctuating photon and carrier densities. These rate equations (Ahmed et al. 2014) are augmented with Langevin noise sources to study the effect of optical feedback. Cross gain saturation and gain recovering coefficients are used to incorporate polarization noise in VCSEL. The resulting photon number p_1, p_2 and carrier densities c_1, c_2 values are used to calculate the output power of the LASER. Where I is the driving current.

$$\frac{dc_1}{dt} = \frac{I}{qV_1} - \frac{c_1}{\tau_e} - [\Gamma_1 p_1 + \Gamma_2 p_2]\frac{g_1}{V_1}, \qquad (1)$$

$$\frac{dc_2}{dt} = \frac{I}{qV_2} - \frac{c_2}{\tau_e} - [(1-\Gamma_1)p_1 + (1-\Gamma_2)p_2]\frac{g_2}{V_2}, \qquad (2)$$

$$\frac{dp_1}{dt} = \left[\Gamma_1 g_1 + (1 - \Gamma_1)g_2 - \frac{1}{\tau_{p1}}\right]S_1 + \frac{k_{tot}n_{sp}}{\tau_{p1}} + LN_1,$$

(3)

$$\frac{dp_2}{dt} = \left[\Gamma_2 g_1 + (1 - \Gamma_2)g_2 - \frac{1}{\tau_{p2}}\right]S_2 + \frac{k_{tot}n_{sp}}{\tau_{p2}} + LN_2,$$

(4)

the gain of LP01 and LP11 modes is given by

$$g_1 = g_{1L}[1 - k_s(\Gamma_1 p_1 + \Gamma_2 p_2)](1 - \epsilon_{22}p_2 - \epsilon_{21}p_1), \quad (5)$$

$$g_2 = g_{2L}[((1 - \Gamma_1)p_1 + (1 - \Gamma_2)p_2)](1 - \epsilon_{11}p_1 - \epsilon_{12}p_2). \quad (6)$$

The linear gain is defined as

$$g_{1L} = v_g \frac{d}{L}a_0(c_1 - ntr) \quad (7)$$

$$g_{2L} = v_g \frac{d}{L}a_0(c_2 - ntr) \quad (8)$$

$$V_1 = \pi r_1^2 d \quad (9)$$

$$V_2 = \pi r_2^2 d \quad (10)$$

2.1 Modulation

2.1.1 Single-tone modulation

To modulate a signal I_b which is to be fed as input to VCSEL. A sinusoidal function is added to the signal with a different frequency. This is the modulating frequency f_m. The amplitude of the signal is I_m. So, the final equation for input current is given by

$$I(t) = I_b + I_m \sin(2\pi f_m t). \quad (11)$$

The modulaton index m can be calculated as m=I_m/I_b.

2.1.2 Two-tone modulation

For two-tone modulation, two sinusoidal signals with operating frequencies f_{m1} & f_{m2} are added to the driving current I_b. The resulting equation of the input bias for dual tone modulation can be represented as:

$$I(t) = I_b + I_m[\sin(2\pi f_{m1}t) + \sin(2\pi f_{m2}t)]. \quad (12)$$

The output power P of emitted light is calculated from the total photon number, $p = p_1 + p_2$, using the formula (Mahmoud et al. 2013)

$$\text{Power} = h\nu \times \frac{(1/2L)\ln(1/R_f)}{\alpha + (1/2L)\ln(1/R_f R_b)\tau_p} \times p, \quad (13)$$

Table 1 Essential parameters and their values

Symbol	Parameter	Value
λ	Emission wavelength	850 nm
D	Thickness of active layer	24 nm
L	Effective cavity length	1000 nm
r_1	Radius of mode LP01 zone	4000 nm
r_2	Radius of active region	7500 nm
k_{tot}	Enhancement factor	1.0
n_{sp}	Inversion factor	2.0
k_s	Gain compression coefficient	8.6×10^{-7}
v_g	Group velocity	8.36×10^4cm/s
a_0	Differential gain	3.50×10^{-2}cm^2
N_t	Transparent carrier density	1.33×10^{-3}cm^{-3}
τ_{p1}	Photon lifetime of mode 1	2 ps
τ_{p2}	Photon lifetime of mode 2	1.88 ps
τ_e	Carrier lifetime	3×10^3 ps
R_f	Reflectivity of the front mirror	0.9991
R_b	Reflectivity of the back mirror	0.9998
α	Material loss of the active layer	1×10^{-6} m^{-1}
λ_1	First modulation wavelength	1510 nm
λ_2	Second modulation wavelength	1550 nm
Γ_1	Confinement factor for mode 1	0.63
Γ_2	Confinement factor for mode 2	0.35
ϵ_{11}	Self gain saturation coefficient for mode 1	2×10^7
ϵ_{12}	Cross gain saturation coefficient for mode 1	0.5×10^7
ϵ_{22}	Self gain saturation coefficient for mode 2	2×10^7
ϵ_{21}	Cross gain saturation coefficient for mode 2	0.5×10^7

where L length of active region, hν photon energy, R_f front mirror reflectivity, R_b rear mirror reflectivity and τ_p photon lifetime

2.2 Numerical calculations

Runge Kutta fourth order method is used to integrate the rate equations. All the values of parameters required for this step are included in the Table 1. Langevin noise sources LN1 and LN2 are generated at every iteration using the formulas (Ahmed et al. 2014) listed below:

$$LN_1(t) = \sqrt{\frac{2 \times k_{tot} \times n_{sp} \times p_1}{\tau_{p_1}} \times x}, \qquad (14)$$

$$LN_2(t) = \sqrt{\frac{2 \times k_{tot} \times n_{sp} \times p_2}{\tau_{p_2}} \times x}, \qquad (15)$$

where x is a random no. generated between $(-1:1)$ with zero mean and unity variances.

2.2.1 Runge Kutta method

To integrate photon and carrier rate equations an algorithm is written for integrating four functions simultaneously.

- The first slope S_1 is calculated at the beginning of step with the help of the boundary conditions provided (value of function at $t = 0$).
- Second slope S_2 is calculated at midpoint of the step size and the first slope value is added to the boundary condition.
- Third slope S_3 is also calculated at mid point of step size but this time second slope is added to the boundary condition.
- Now, we use the third slope for evaluating the fourth slope S_4 at the endpoint of step size. Now all these slopes are combined using the equation stated below to get the value at the step size.

$$y(t+h) = y(t) + \frac{S_1 + 2 \times S_2 + 2 \times S_3 + S_4}{6} \times h, \quad (16)$$

where $y(t + h)$ is the desired result $y(t)$ is the result at previous step S_1, S_2, S_3, S_4 are the slopes h step size In Runge Kutta fourth order method, a step size is divided into four parts and the slope of the function is calculated at each step then a weighted sum of all the slopes is used to get the final estimate. Hence using four slopes to calculate the value at a single step size enhances the accuracy of the results.

3 Result and analysis

In this paper, output power of VCSEL is calculated, firstly when noise is considered in the system and lastly when the system is assumed to be noiseless. Further the VCSEL model is subjected to CW and two-tone modulation techniques. In Fig. 1, the graphs are obtained between output power and simulation time for modes LP01 and LP11.

LP01 is known as the fundamental mode of travelling. In the graph above we depict a trade-off between the output power and the time when subjected to two-tone modulation
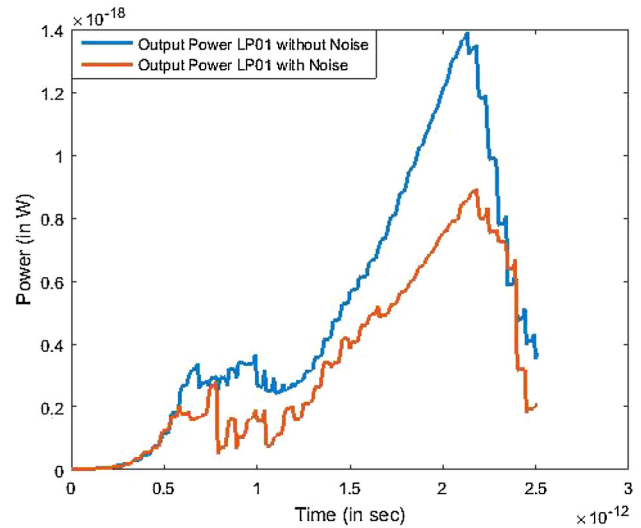
Fig. 1 Comparative two-tone modulation LP01

scheme. The blue graph refers to the output power vs time of VCSEL without noise while the other graph depicts the output power vs time of VCSEL with noise. The graph which has no noise added to it shows a rise in output power for the positive slope of bias and it falls for the negative slope of bias. Fluctuations are seen throughout the time interval due to the modulating signal. In two tone modulation model, the saturation in output power is seen in the interval 0.5–1 ps, after which the output power again starts rising. After attaining the maximum value of the output power, it is seen that there is a rapid decrease in the output power. Both the graph shows a repetitive characteristic even for the next cycle of simulations to come. Now for the graph with noise, introduction of various noises such as polarization and spontaneous noise has been done. While considering noise as a factor, the amplitude of the output power for the one with additive noise shows more reduction in the values at specific time intervals when compared with the graph which has no addition of noise. It can be concluded that the noises which is added, causes a reduction in the output power of VCSEL. The graphical analysis clearly show that the fluctuations tend to increase when the noises are added in VCSEL rate equations. Fluctuations have a direct proportion relationship with the amplitude of the output power of LASER. For the positive cycle of bias, there is an exponential increase in the amplitude of output power and as we stated above the amplitude of the fluctuations tend to increase with rising amplitude of power. With the addition of noise, the fluctuations in the output power are more random and have more effect on the amplitude of output power. As the simulation time increases, we observe a negative slope of bias. If the negative slope maintains for a short interval then the graph tends to saturate, and if the slope sustains for long then we see a downfall in the amplitude of output power.
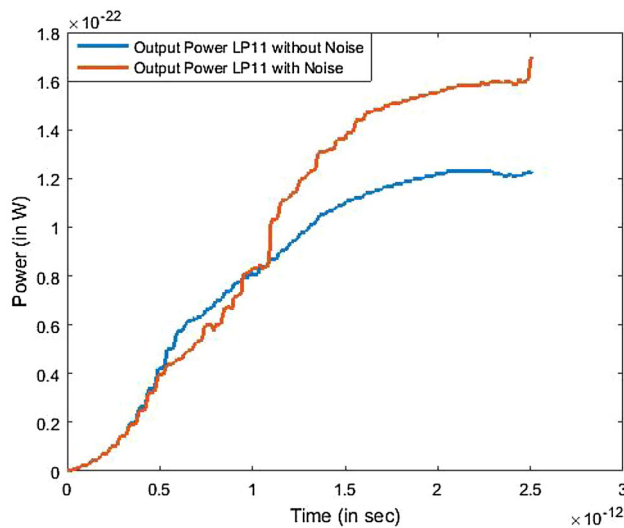
Fig. 2 Comparative two-tone modulation LP11

Fig. 3 Comparative continuous wave modulation

Fig. 4 Comparative continuous wave modulation

In the two-tone modulation scheme the next mode upon which the analysis have been done is for the secondary mode represented by LP11. Figure 2, depicts the output power vs time with and without noise for the secondary mode of travelling. LP11 has a lower amplitude of the output power as compared to the fundamental mode of travelling, i.e. LP01. The fluctuations show less effect on the amplitude of the output power as compared to the LP01 model. This can be explained by the fact that noise factor is directly proportional to the amplitude of the travelling wave. The graph in the secondary mode increases exponentially with the positive slope of bias and for the negative slope of bias the graph does not show an exponential decrease due to of the presence of previously generated carriers which are able to support the amplitude of the output power because of the low amplitude of power in secondary mode. In the time interval between 2 and 2.5 ps, one can observe a rapid reduction in the output power of the fundamental mode after attaining its maximum value. When the same interval is observed for secondary mode there is no such reduction in the amplitude of the output power. It happens because the amplitude of power in secondary mode is very low and previously generated carriers are able to support the output power's amplitude. Hence instead of the decrease in amplitude one can observe that the amplitude of output power saturating in the interval mentioned above. Due to the low amplitude of output power it approximately matches the noise amplitude hence the amplitude of resulting power seems to be increasing.

The comparative plot of the output power of VCSEL vs time shown in Fig. 3 for the mode LP01 when subjected to CW modulation. The trade-off between the output power and time is exponentially smooth throughout the time of simulation. One can see an exponential growth in the output power because the input is a continuous wave, the output power
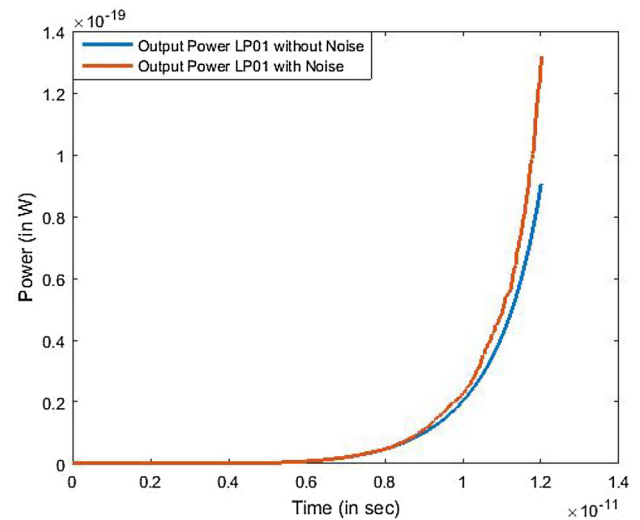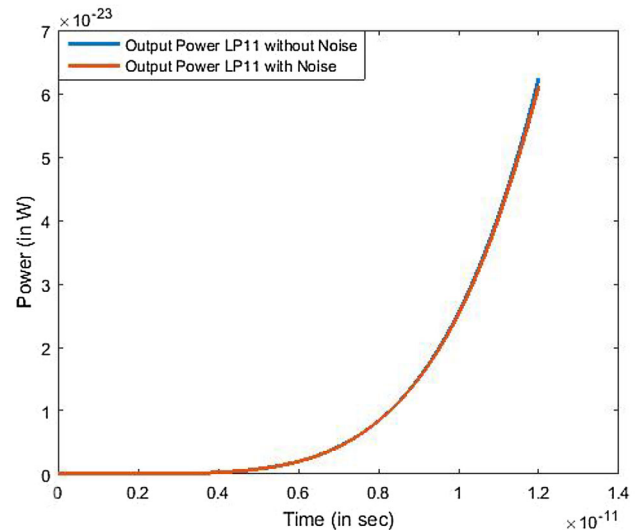
doesn't show much fluctuations when the noise is added. Although when there is an exponential increase in the slope of graph, some minor fluctuations can also be noted. These fluctuations are not large enough to effect the performance of VCSEL. Hence, these fluctuations can be ignored in the case of CW modulation for the mode LP01.

In the mode LP11, as seen in Fig. 4, the effect of noise is almost negligible. The trade-off between the output power and the time is almost same for both the graphs over the whole simulation time. The fluctuations in mode LP11 are so small that they don't effect the output power of the LASER. Thus much change can not be seen in the nature of the above graphs.
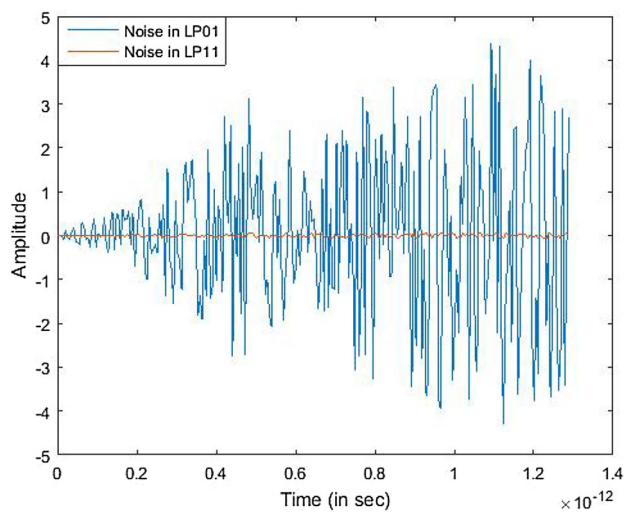
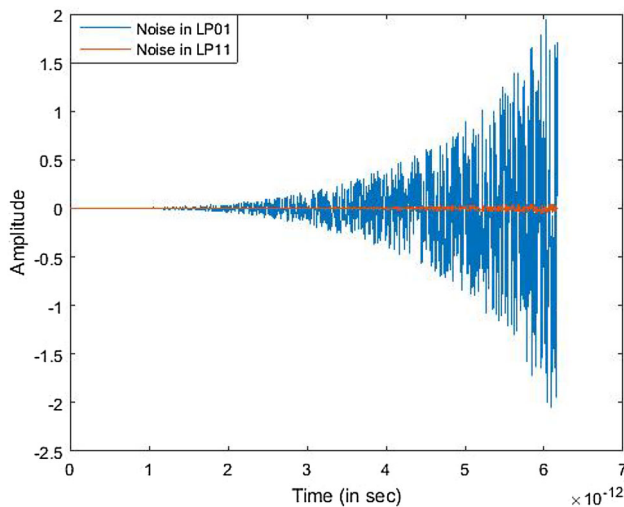**Fig. 5** Comparative noise in two-tone modulation

Fig. 6 Comparative noise in continuous wave modulation

The comparative plots of noise generated in the two modes for both the modulation techniques are given in Figs. 5 and 6 respectively.

4 Conclusion

The characteristics of output power of VCSEL are studied under different conditions, including two-tone modulation and CW operation once without the addition of noise and once when internal noises are considered. By analyzing the graphs which include noise as a factor in both modes and under different modulation schemes, one can conclude that the internal noises being studied are directly proportional to the amplitude of output. In CW modulation, there are very minute effects of noise on the output as the input is linear.

Mode LP01 being the dominant mode has more power compared to the secondary mode LP11. Hence the fluctuations due to noise in mode LP01 are higher than mode LP11.

In case of two-tone modulation, the input bias is changing rapidly and nature of graph as observed in the output is corresponding to the slope of bias. If the slope of bias starts decreasing for a short period then stimulated emission and population inversion are able to balance the output power. Hence the power doesn't decrease for that interval and just saturates. If the bias tends to decrease continuously for a longer period then there are not much carriers left in the cavity to support the output power and the amplitude of output power falls. So one can conclude that VCSEL is able to handle sudden losses in input bias for a short period but the output power degrades if the loss in input sustains for long. The influence of noise generated due to the spatial distribution of carriers along with polarization noise and spontaneous noise on output power of VCSEL would be the field of future research.

Compliance with ethical standards

Conflict of interest The author states that there is no conflict of interest.

References

Ahmed M, Yamada M (2012) Mode oscillation and harmonic distortions associated with sinusoidal modulation of semiconductor lasers Mode oscillation and harmonic distortions associated with sinusoidal modulation of semiconductor lasers. Eur Phys J D 66:246–246. https://doi.org/10.1140/epjd/e2012-30229-7

Ahmed M, Mahmoud SWZ, Hassan A (2014) Modeling and simulation of VCSELs noise and its influence on noise performance of RF fiber links. Opt Laser Technol 56:375–381. https://doi.org/10.1016/j.optlastec.2013.09.024

Chen YC, Liu JM (1987) Polarization bistability in semiconductor laser: rate equation analysis. Appl Phys Lett 50(20):1406–1408. https://doi.org/10.1063/1.97835

Choquette KD, Richie DA, Leibenguth RE (1994) Temperature dependence of gain guided vertical cavity surface emitting laser polarization. Appl Phys Lett 64(16):2062–2064. https://doi.org/10.1063/1.111737

Gatare I, Sciamanna M, Buesa J, Thienpont H, Panajotov K (2005) Polarization switching and dynamics induced by optical injection in VCSELs. In: EQEC '05. European quantum electronics conference, Munich, 2005, p 125. https://doi.org/10.1109/EQEC.2005.1567296

Goyal P, Sharma M, Jha A, Kumari M, Singh SP, Singh N, Kaur G (2016) Design and analysis of VCSEL LASER for third window of optical communication system. In: Electrical, electronics, and optimization techniques (ICEEOT), international conference on. IEEE, pp 4220–4224. https://doi.org/10.1109/ICEEOT.2016.7755512

Lee HLT, Ram RJ (2001) Mode partition noise in vertical cavity surface emitting lasers. In: 2001 digest of LEOS summer topical meetings: advanced semiconductor lasers and applications/ultraviolet and

blue lasers and their applications/ultralong haul DWDM transmission and networking/WDM compo, Copper Mountain, CO, USA, p 2.https://doi.org/10.1109/LEOSST.2001.941888

Mahmoud SWZ, Ahmed M, Hassan AMA (2013) Comprehensive large-signal analyses of RF modulation of vertical cavity surface emitting lasers. Opt Laser Technol 45:406–413. https://doi.org/10.1016/j.optlastec.2012.06.016 (ISSN 0030-3992)

Mukaihara T, Ohnoki N, Hayashi Y, Hatori N, Koyama F, Iga K (1995) Excess intensity noise originated from polarization fluctuation in vertical-cavity surface-emitting lasers. IEEE Photonics Technol Lett 7(10):1113–1115. https://doi.org/10.1109/68.466560

Quirce A, Valle A, Gimenez C, Pesquera L (2011) Intensity noise characteristics of multimode VCSELs. J Lightwave Technol 29(7):1039–1045. https://doi.org/10.1109/JLT.2011.2112754